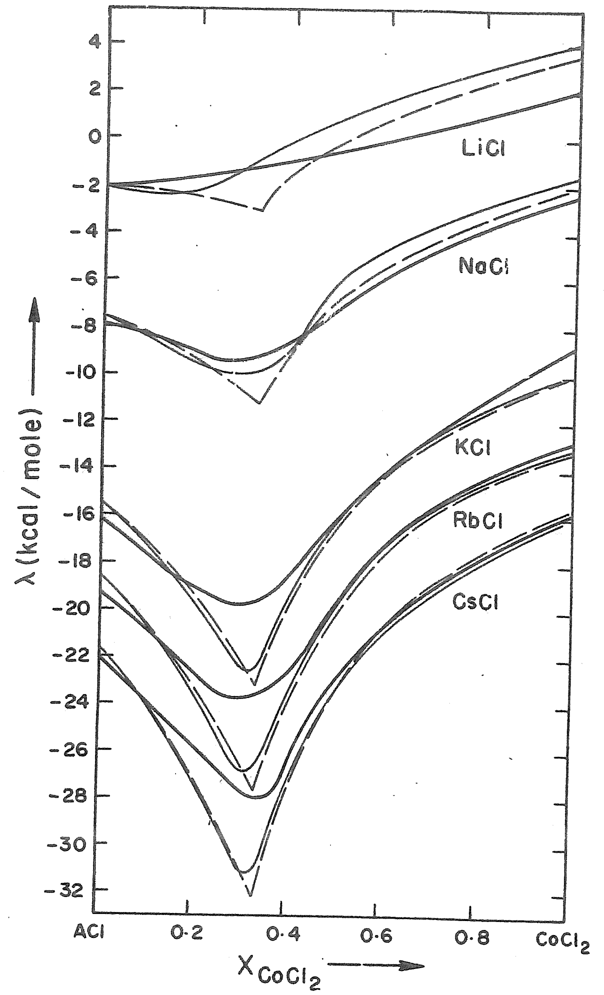

FIG. 2. Interaction parameters in $CoCl_2$–ACl systems ═══ Experimental (8). - - - From model for complete complexing. ——— From model for partial dissociation.

Since the pressure–volume work of mixing is negligible, the molar enthalpy of mixing, ΔH, may be taken to be equal to the change in internal energy on mixing. Still under the assumption of complete complexing, that part of the enthalpy of mixing resulting from complex formation is now given by

$$[5] \quad \Delta H = X_{MY_2}\Delta e - \frac{X_{MY_2}}{2}\Delta e_1 \qquad [X_{MY_2} \leqslant 1/3]$$

$$[6] \quad \Delta H = \left(\frac{2X_{MY_2} + X_{AY}}{4}\right)\Delta e - \frac{X_{MY_2}}{2}\Delta e_1 \qquad [X_{MY_2} \geqslant 1/3]$$

where Δe is given by eq. 4. For $X_{MY_2} \leqslant 1/3$, $N_{A^+} = 1$, and $N_{M^{2+}} = 0$. For $X_{MY_2} \geqslant 1/3$, N_{A^+}

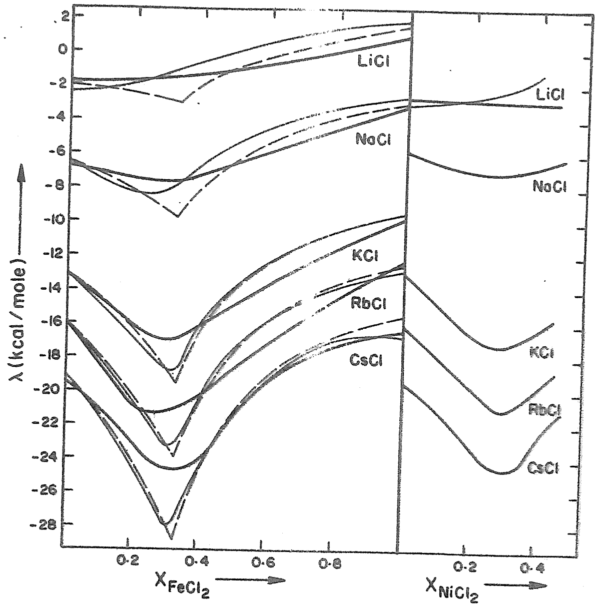

FIG. 3. Interaction parameters in $FeCl_2$–ACl and $NiCl_2$–ACl systems. ═══ Experimental (7, 8). - - - From model for complete complexing. ——— From model for partial dissociation.

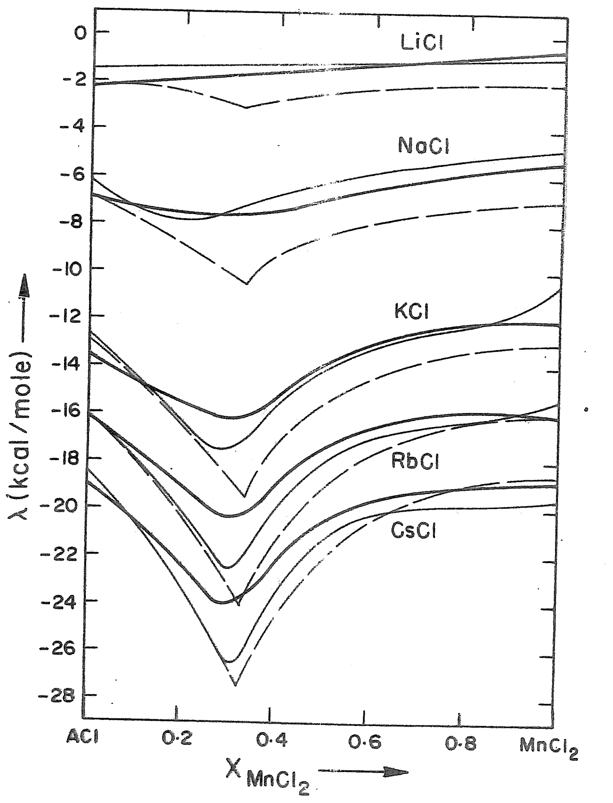

FIG. 4. Interaction parameters in $MnCl_2$–ACl systems. ═══ Experimental (8). - - - From model for complete complexing. ——— From model for partial dissociation.

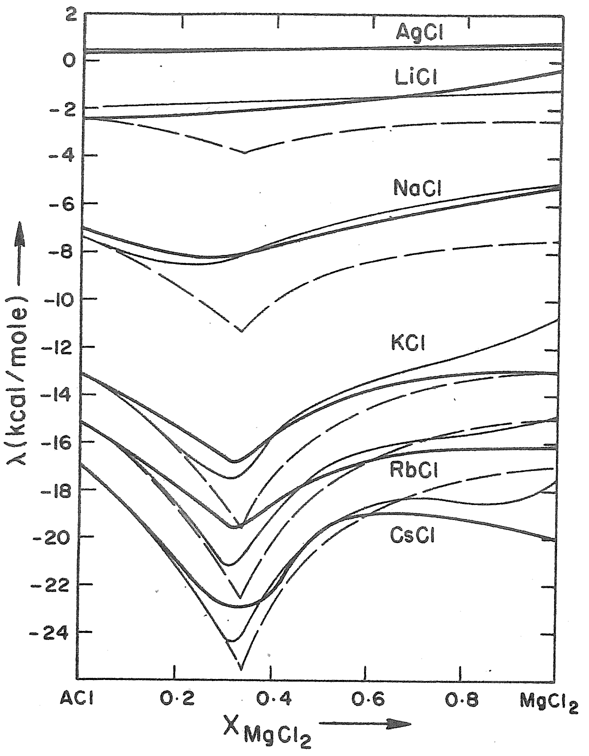

FIG. 5. Interaction parameters in $MgCl_2$–ACl systems. ——— Experimental (3). - - - From model for complete complexing. ——— From model for partial dissociation.

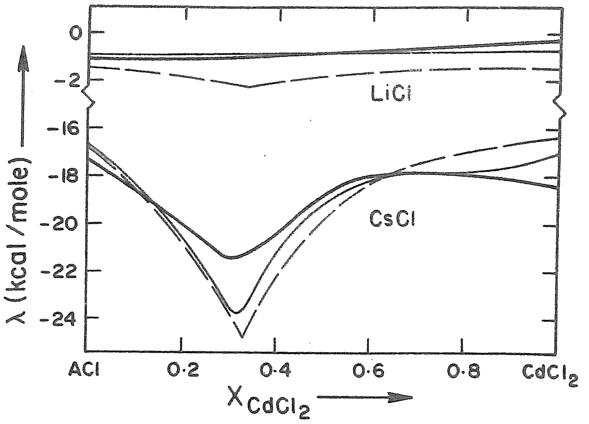

FIG. 6. Interaction parameters in $CdCl_2$–ACl systems. ——— Experimental (9). - - - From model for complete complexing. ——— From model for partial dissociation.

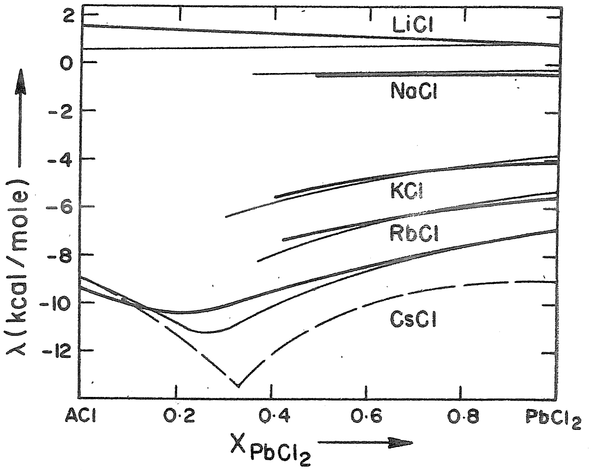

FIG. 7. Interaction parameters in $PbCl_2$–ACl systems. ——— Experimental (10). - - - From model for complete complexing. ——— From model for partial dissociation.

$= 4X_{AY}/(3 - X_{MY_2})$, and $N_{M^{2+}} = (1 - N_{A^+})$ (see Table 1). Making the substitutions in eqs. 5 and 6 and simplifying, the following equations for the case of complete complexing result

$$[7] \quad \Delta H = \frac{X_{MY_2}}{2} b_1 + X_{MY_2} b_2 \qquad [X_{MY_2} \leqslant 1/3]$$

$$[8] \quad \Delta H = \frac{X_{AY}}{4} b_1 + \frac{X_{AY}(1 + X_{MY_2})}{(3 - X_{MY_2})} b_2 \qquad [X_{MY_2} \geqslant 1/3]$$

where b_1 and b_2 are defined as

$$[9] \quad b_1 = \Delta e_1$$

$$[10] \quad b_2 = (\Delta e_2 - \Delta e_1)$$

The parameter b_1 is independent of concentration, and is a property only of the salt MY_2. It is independent of the particular MY_2–AY system. The parameter b_2 has one concentration-independent value for each MY_2–AY system. The first terms in eqs. 7 and 8 are the same as eqs. 2 and 3. The final terms in eqs. 7 and 8 give the strengthening (or weakening) effect of the A^+ ions on the complexes, and these terms are shown as the lower curve in Fig. 1*a* (b_2 is taken to be negative in Fig. 1*a*).

The overall interaction parameter which results from the combination of both enthalpy terms is shown in Fig. 1*b*. Let $\lambda_{X=1}$ and $\lambda_{X=0}$ be the values of λ when $X_{MY_2} = 1$ and $X_{MY_2} = 0$, respectively, and let $\Delta\lambda = (\lambda_{X=0} - \lambda_{X=1})$. From Fig. 1*b* it can be seen that $\Delta\lambda = b_1/4$. $\Delta\lambda$ should thus depend only on the salt MY_2, and should be constant within a group of MY_2–AY systems for a given salt MY_2. Furthermore, from the experimental value of $\Delta\lambda$, b_1 can be numerically estimated. The greater is the tendency of a salt MY_2 to form complexes, the more negative should be $\Delta\lambda$.

tems with NaCl and LiCl, $\Delta\lambda$ is somewhat negative, but, as shown later, this is thought to result from dissociation of the complexes. A value of $b_1 = 0.0$ was chosen for all these systems. As shown in Figs. 4–6, this results in reasonable agreement with the experimental data. The values of b_2 used are listed in Table 2.

In these less strongly complexed systems ($b_1 = 0$), the evidence for dissociation of the complexes is very strong in the systems with LiCl and NaCl, and is evident in the systems with KCl also.

For the $MgCl_2$ systems, enthalpies for the system $MgCl_2$–AgCl are available (3), and are shown in Fig. 5. This system is best fitted with $b_2 = +1.5$ kcal. The positive value may result from the fact that Ag has a tendency to form covalent bonds with chlorine and thus has a strong tendency to weaken and break up the complexes.

In the previous publication (5), a value of $b_1 = -3.0$ kcal was chosen to fit the $MgCl_2$ systems. The difference between this and the present value of 0.0 is small enough to make very little difference in the calculated curves.

For the $PbCl_2$–ACl systems (10) in Fig. 7, a value of $b_1 = 0.0$ and values of b_2 as listed in Table 2 were used. These parameters do not give good fits for the case of complete complexing, as can be seen from the dashed line for the $PbCl_2$–CsCl system in Fig. 7. However, as will be discussed later, these values do appear to give good fits when dissociation is taken into account. In the $PbCl_2$ systems there is evidence for dissociation even in the system with CsCl.

In Fig. 8*a* are plotted, as the heavy solid lines, ΔH curves for the BeF_2–LiF and BeF_2–KF systems as obtained calorimetrically by Holm and Kleppa (11). For the BeF_2–LiF system, ΔH is negative for small X_{BeF_2} and positive for large X_{BeF_2}. A plot of λ for this system is shown in Fig. 8*b*, and is of the general shape predicted by the present model. A value of $b_1 = -50$ kcal for BeF_2 gives a good fit to $\Delta\lambda$ for this system. This means that BeF_2 has a very strong tendency to form tetrahedral complexes. With a value of $b_2 = +20$ kcal for the BeF_2–LiF system, the curves calculated for complete complexing are shown as the dashed lines in Figs. 8*a*, *b*. Quite good agreement is obtained. For the BeF_2–KF system, a value of $b_2 = 0.0$ was chosen.

By comparing the fits to ΔH in Fig. 8*a* with the same fits to λ in Fig. 8*b*, it can be appreciated how small discrepancies in agreement between experimental and calculated values of ΔH are greatly magnified in the "interaction parameter" plots. This effect is particularly pronounced near the ends of the curves, as is readily seen in the curves for the BeF_2–KF system. A discrepancy between experimental and calculated values of 1.0 kcal at $X_{MY_2} = 0.9$, say, is magnified to a discrepancy of about 11.0 kcal in the plots of λ. For the chloride systems discussed previously, the interaction parameter plots of Figs. 2–7 similarly magnify discrepancies. The agreement between experiment and model in absolute values of ΔH would be more readily apparent in plots of ΔH than in the plots of λ. However, the important shape factors (the extent of the "dip" at $X_{MY_2} = 1/3$, the value of "$\Delta\lambda$", etc.) can only be seen in plots of λ.

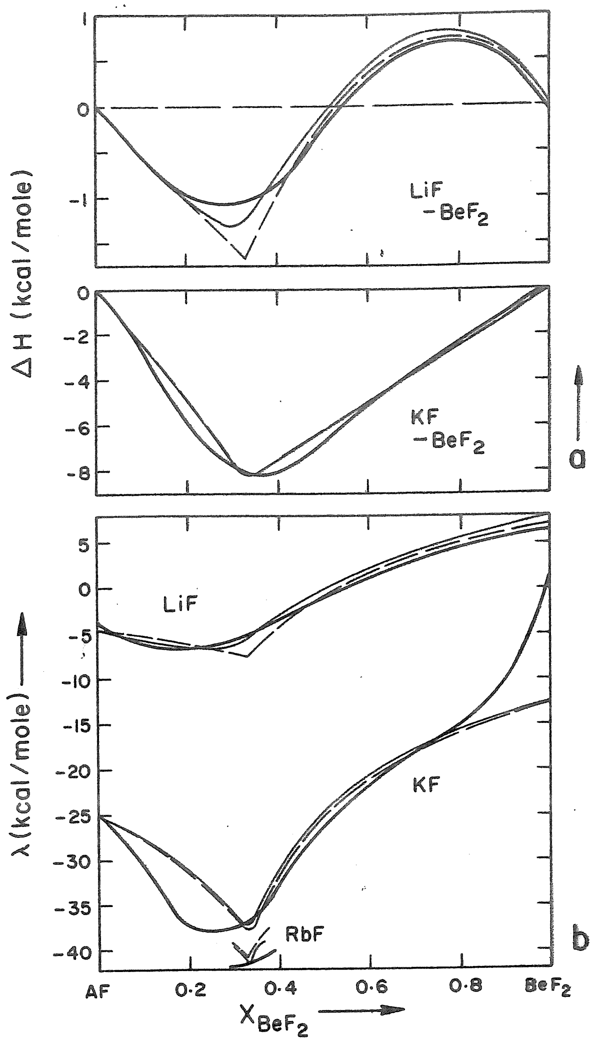

FIG. 8. Enthalpies and interaction parameters in BeF_2–AF systems. ——— Experimental (11). - - - From model for complete complexing. ——— From model for partial dissociation.

Of course, because of evidence of viscosities, electrical conductivities, etc., molten BeF_2 is generally accepted as being polymeric in nature, with BeF_4 tetrahedra sharing corners, and the assumption of discrete BeF_4^{2-} anions and Be^{2+} cations in pure BeF_2 as required by the present model is undoubtedly incorrect. This matter will be discussed at somewhat greater length later. Nevertheless, the very simple model just discussed can give surprisingly good agreement to the enthalpy of mixing data. In particular, for the BeF_2–LiF system, the existence of positive ΔH values in the BeF_2-rich concentration range, and negative values in the LiF-rich range is quite simply treated.

Entropies

The configurational entropy of mixing under the assumption of complete complexing is calculated as follows. For $X_{\mathrm{MY}_2} \leqslant 1/3$, there is only one type of cation, A^+. The configurational entropy is then calculated by assuming a random mixture of the MY_4^{2-} and Y^- anions over $(X_{\mathrm{AY}} - X_{\mathrm{MY}_2})$ anion sites. For $X_{\mathrm{MY}_2} \geqslant 1/3$, only one type of anion, MY_4^{2-}, exists, and a random mixture of the A^+ and M^{2+} cations over the $(3 - X_{\mathrm{MY}_2})/4$ cation sites is assumed. At $X_{\mathrm{MY}_2} = 1/3$, only A^+ cations and MY_4^{2-} anions exist and the configurational entropy is zero. Pure MY_2 contains only M^{2+} cations and MY_4^{2-} anions, and so has zero configurational entropy.

The molar configurational entropy of mixing, ΔS, is shown in Fig. 1*c* as the curve with two "humps". This is the typical sort of curve expected if the "compound" A_2MY_4 is formed, as has been discussed by Østvold (4) and by Østvold and Kleppa (12). The ideal (Raoultian) entropy of mixing is also shown in Fig. 1*c*.

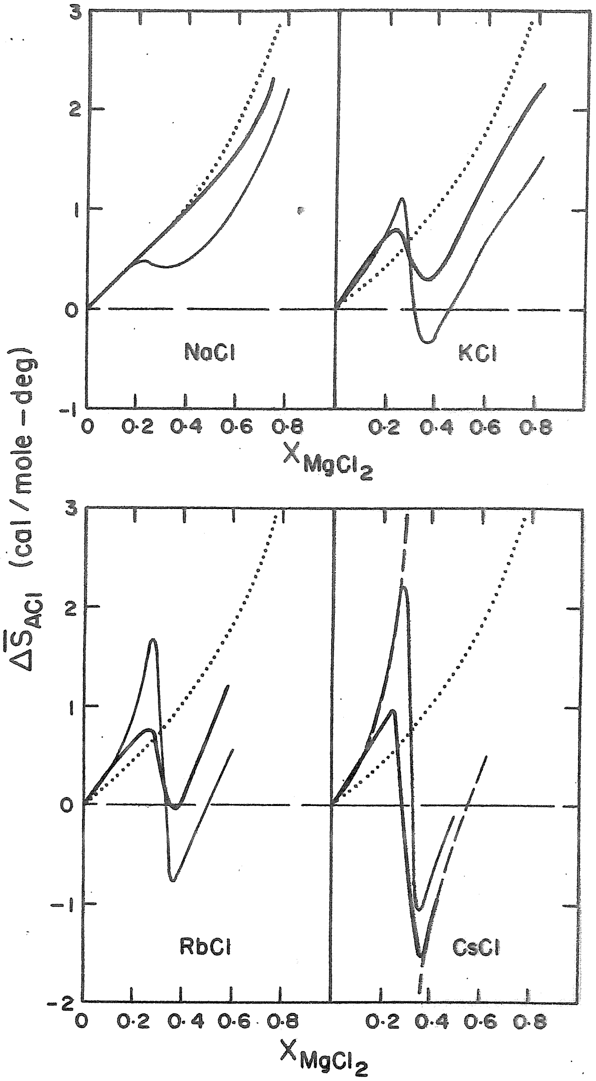

FIG. 9. Partial molar entropies of mixing of alkali chloride in $MgCl_2$–ACl systems. ═══ Experimental (4). - - - From model for complete complexing. ——— From model for partial dissociation. ···· Ideal (Raoultian).

Experimental partial molar entropies of mixing, $\Delta \bar{S}_{\mathrm{ACl}}$, of ACl in the $MgCl_2$–ACl systems are shown in Fig. 9. These curves were obtained by Østvold (4), who measured the e.m.f. of concentration cells with glass membranes and combined his data with the partial enthalpies calculated from the calorimetric data (3). The ideal partial entropies, $-R \ln X_{\mathrm{ACl}}$, are also shown in Fig. 9. The experimental curves show positive deviations from ideality for solutions concentrated in ACl, and then, near $X_{\mathrm{MgCl}_2} = 1/3$, there is a rapid change to negative deviations. From the integral entropy of mixing curve in Fig. 1*c* it can be appreciated that this is qualitatively the predicted behavior of the partial entropy. In Fig. 9, in the graph for the system with CsCl, the dashed line is $\Delta \bar{S}_{\mathrm{ACl}}$ as calculated for complete complexing. The predicted effect at $X_{\mathrm{MgCl}_2} = 1/3$ is, of course, too drastic. As the A^+ cations become smaller, the experimentally observed effect at $X_{\mathrm{MgCl}_2} = 1/3$ becomes less and less pronounced, again suggesting, as discussed by Østvold (4), that dissociation of the complexes occurs.

In Fig. 10 are partial excess entropies of mixing of $MnCl_2$, $\Delta \bar{S}^{\mathrm{E}}_{\mathrm{MnCl}_2}$, in $MnCl_2$–ACl systems, as calculated by Kucharski and Flengas (13) from the temperature dependences of the e.m.f.s of formation cells, The dashed line in the graph for the system with CsCl is the curve predicted from the model for complete complexing. Positive values of $\Delta\bar{S}^{E}_{MnCl_2}$ are predicted for $X_{MnCl_2} > 1/3$, with a sudden change to negative values for $X_{MnCl_2} < 1/3$. This is in quite good agreement with the experimental curve for the $MnCl_2$–$CsCl$ system. For smaller alkali cations, the experimentally observed effect at $X_{MnCl_2} = 1/3$ becomes less and less pronounced, again suggesting that dissociation of the complexes occurs.

Kucharski and Flengas (13) discussed the results in Fig. 10 using a similar model which was based upon the assumption of $MnCl_4{}^{2-}$ complexes, and which assumed complete complexing. They also included an additional term to account for vibrational entropy effects.

Discrete Complex Anion Model, Partial Dissociation

A complete discussion of the treatment of partial dissociation in the discrete complex anion model has been given previously (5).

Reaction 1 is not displaced completely to the right as was assumed in the case of complete complexing, and instead, an equilibrium is set up, with a fraction ($\alpha/2$) of the total M existing in $MY_4{}^{2-}$ anionic complexes, and a fraction ($1 - \alpha/2$) existing, for the purposes of statistical calculations, as free M^{2+} cations. The amounts of the various ionic species in a mole of solution are given as functions of α in column 4 of Table 1.

Let α_{max} be the maximum permissible value of α. For $X_{MY_2} \leqslant 1/3$, $\alpha_{max} = 2$, and is that value of α for which all M is complexed. For $\alpha = 2$, column 4 of Table 1 reduces to column 2. For $X_{MY_2} \geqslant 1/3$, $\alpha_{max} = (1 + X_{MY_2})/2X_{MY_2}$, and is that value of α (see ref. 5) for which all the Y is complexed. With $\alpha = (1 + X_{MY_2})/2X_{MY_2}$, column 4 of Table 1 reduces to column 3. For $X_{MY_2} = 1$, for instance, $\alpha_{max} = 1$, and one half of the M is complexed when complete complexing occurs in pure MY_2.

The molar configurational entropy, S, of the solution at any composition is written by assuming a Temkin solution of M^{2+} and A^+ cations and of Y^- and $MY_4{}^{2-}$ anions. This gives S as a function of α and of composition, $S(\alpha,X)$.

Self-association of pure MY_2 must also be considered. The fact that no such model for complexing in molten salts can be thermodynamically consistent without the consideration of self-association of the pure components was first pointed out by Braunstein (14). If α^0 is the value of α in pure MY_2, then $S^0_{MY_2}$, the molar configurational entropy of pure MY_2, may be written as a function of α^0, $S^0_{MY_2}(\alpha^0)$, assuming a Temkin solution of the three ionic species M^{2+}, $MY_4{}^{2-}$, and Y^-. For $\alpha^0 = \alpha^0_{max} = 1$, for instance, complete complexing occurs. In this case there are only M^{2+} and $MY_4{}^{2-}$ species in pure MY_2, and $S^0_{MY_2} = 0$ as discussed earlier.

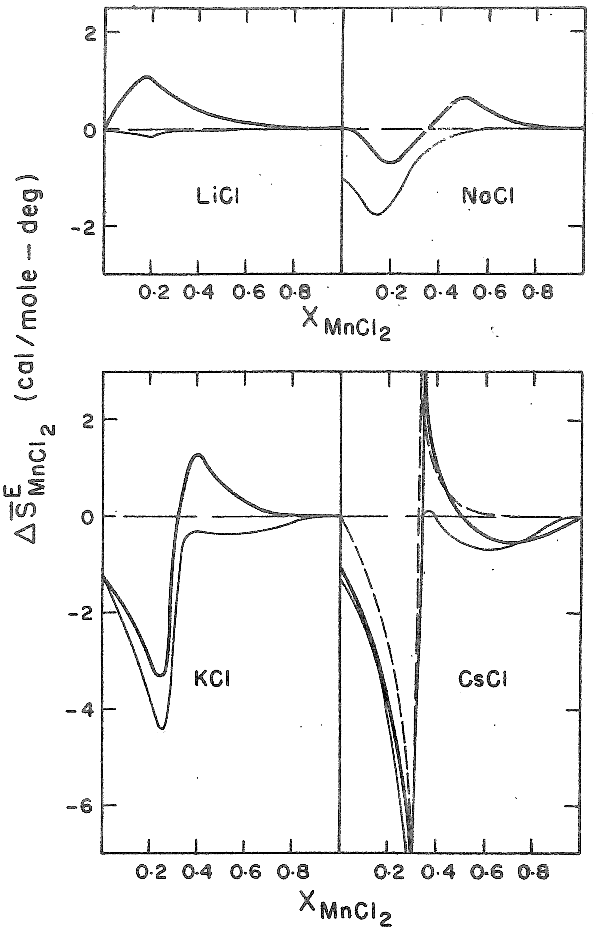

FIG. 10. Partial molar excess entropies of mixing of $MnCl_2$ in $MnCl_2$–ACl systems. ═══ Experimental (13). - - - From model for complete complexing. ——— From model for partial dissociation.

The configurational entropy, S^0_{AY}, of pure AY is zero, and so the molar configurational entropy of mixing, ΔS, is given as a function of α, α^0, and composition

$$[11] \quad \Delta S(\alpha,\alpha^0,X) = S(\alpha,X) - X_{MY_2}S^0_{MY_2}(\alpha^0)$$

The explicit function has been given previously (5). For complete complexing, with $\alpha = \alpha_{max}$ and $\alpha^0 = 1$, the equation for ΔS reduces to the curve